

# 1,4-Alkyl migration associated with simultaneous S–C bond cleavage and N–C bond formation in platinum complexes of 2-aminothioethers. Characterization of intramolecular interligand charge transfer phenomenon†

Sutanuva Mandal,<sup>a</sup> Nandadulal Paul,<sup>a</sup> Priyabrata Banerjee,<sup>a</sup> Tapan K. Mondal<sup>b</sup> and Sreebrata Goswami<sup>\*\*</sup>

Received 4th September 2009, Accepted 22nd December 2009

First published as an Advance Article on the web 2nd February 2010

DOI: 10.1039/b918336a

Chemical reactions of Pt(pap)Cl<sub>2</sub> [pap = 2-(phenylazo)pyridine] with the N,S-donor atom ligands, 2-alkylthioanilines (HL, (H<sub>2</sub>N^SR), where R = Me, -CH<sub>2</sub>Ph, -CH<sub>2</sub>-CH=CH<sub>2</sub>) in acetonitrile solvent under alkaline conditions yielded mixed chelate donor–acceptor complexes, [Pt(pap)(HN^SR)]<sup>+</sup> (**1**<sup>+</sup>, R = Me), [Pt(pap)(HN^AS)] (**2**, HN^AS = 2-amidothiophenolate, R = Me, -CH<sub>2</sub>Ph, -CH<sub>2</sub>-CH=CH<sub>2</sub>) and [Pt(pap)(RN^AS)] (RN^AS = 2-(N-alkyl)amidothiophenolate **3** and **4**, R = -CH<sub>2</sub>Ph, -CH<sub>2</sub>-CH=CH<sub>2</sub>). Unusual types of 1,4-alkyl group migration associated with simultaneous S–C bond cleavage and N–C bond formation were observed for R = -CH<sub>2</sub>Ph, -CH<sub>2</sub>-CH=CH<sub>2</sub>. However, for R = Me, only S–C bond cleavage occurred producing compound **2** at a higher temperature. Under identical experimental conditions the reaction of Pt(bpy)Cl<sub>2</sub> [bpy = 2,2'-bipyridine] with 2-methylthioaniline afforded [Pt(bpy)(HN^SR)]<sup>+</sup> (**5**<sup>+</sup>, R = Me) as the only product with no S–C bond activation. The complexes have been characterized by <sup>1</sup>H NMR, UV-vis-NIR, ESI-MS, EPR and cyclic voltammetry studies. Single-crystal X-ray structures of the complexes, [**1**][OTf] (OTf = trifluoromethanesulfonate), **2**, **3**, **4** and [**5**][OTf] are reported. The Pt-pap complexes (**1**<sup>+</sup> and **2–4**) showed intense interligand charge transfer (ILCT) transition in the NIR-region (>800 nm). This band in the Pt-bpy analogue, [**5**]<sup>+</sup> shifted to a much higher energy, at 545 nm. The cationic complex, [**1**][OTf] displayed two reversible responses at –0.21 and –0.94 V along with two irreversible anodic responses at 0.48 and 0.90 V. The molecular compounds, **2**, **3** and **4** showed two reversible waves near –0.60 and –1.30 V and an irreversible anodic response near 0.5 V. The response at the anodic potential is presumably due to oxidation of 2-amidothioether/2-amidothiophenolate ligand while the reversible responses at cathodic potentials are due to successive reductions of the azo chromophore of the coordinated pap ligand. The redox processes are characterized by EPR and spectroelectrochemistry. Density-functional theory calculations were employed to confirm the structural features and to support the spectral and redox properties of the complexes.

## Introduction

In this work we have studied the reaction of Pt(pap)Cl<sub>2</sub> [pap = 2-(phenylazo)pyridine] and 2-alkylthioanilines (Chart 1) in an attempt to prepare mixed ligand donor–acceptor platinum complexes of pap and the aminothioether ligands. Over the past three decades a vast literature has built up around mixed ligand complexes of platinum metal, particularly Pt(diimine)(dithiolate) systems.<sup>1</sup> The Pt atom in these examples links the ligands that exhibit donor–acceptor qualities to each other and the low energy charge transfer transitions characterize<sup>2</sup> these complexes. We

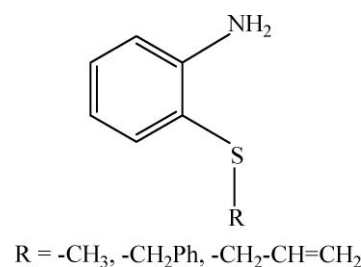


Chart 1

<sup>a</sup>Department of Inorganic Chemistry, Indian Association for the Cultivation of Science, Kolkata, 700 032, India. E-mail: icsg@iaes.res.in; Fax: +91-33-24732805

<sup>b</sup>Department of Chemistry, Jadavpur University, Kolkata, 700032, India

† Electronic supplementary information (ESI) available: X-ray crystallographic files in CIF format for [**1**][OTf], **1**, **3**, **4** and [**5**][OTf]; figures of ESI-MS and <sup>1</sup>H NMR of [**1**]Cl, **2**, **3**, **4** and [**5**]Cl; ORTEP and atom numbering scheme of [**1**][OTf], **2**, **3**, **4** and [**5**][OTf]; DFT and TD DFT calculations of [**1**]Cl, **2**, **3** and [**5**][OTf]; EPR spectra of electrogenerated **1**, **2**<sup>•-</sup>, **3**<sup>•-</sup>, **4**<sup>•-</sup> in CH<sub>3</sub>CN/0.1 M Et<sub>4</sub>NClO<sub>4</sub>. CCDC reference numbers 746833–746837. For ESI and crystallographic data in CIF or other electronic format see DOI: 10.1039/b918336a

have used two redox non-innocent ligands of opposite character because of the following reasons. The azoaromatic ligand (pap) was chosen for its potent π-acceptor ability<sup>3</sup> and its superior acceptor ability over a diimine ligand like 2,2'-bipyridine is now well established. Such Pt-complexes containing pap as the acceptor ligand may be anticipated to constitute charge transfer molecules with absorption in the long wavelength (red) region. Redox active molecules that absorb intensely in the red region attract interest as functional materials.<sup>4</sup> Selection of the 2-alkylthioaniline as a donor was originated from our recent interest in quinone related ligand

systems.<sup>5</sup> In the present context it is worth noting that coordination of the 2-amidothiophenolate ligand and its redox partners has been elaborated over recent years and N-substituted 2-amidothiophenolate ligands have been the focus of several studies.<sup>6</sup> In comparison, the corresponding coordination chemistry of 2-aminothioether ligands has not been addressed<sup>7</sup> systematically. Moreover, we recently have noted<sup>8</sup> some unexpected chemical reactions of the coordinated aminothioether ligands in their ruthenium complexes. Similar chemical reactions *via* activation of the S–C bond were envisaged in the pap containing Pt-complexes of the aminothioether ligand. In passing we also wish to note that in the active site of Galactose Oxidase enzyme, a single Cu(II) is coordinatively bound to thioether modified tyrosyl radical.<sup>9</sup>

The reference chemical reactions have resulted in an unprecedented type of 1,4-migration of the alkyl group from sulfur (thioether function) to nitrogen (anilido nitrogen function) in the coordinated 2-amidothioether ligands. This transformation is associated with simultaneous S–C bond rupture and N–C bond formation reactions. The S–C bond rupture processes are important in the context of developing mechanistic knowledge to desulfurization technology<sup>10</sup> and to biological pathways such as alkyl transfer<sup>11</sup> *etc.* Two principal pathways *viz.* homolytic and heterolytic bond cleavage reactions are discussed in the literature.<sup>11,12</sup> The chemical reactions, studied herein, are followed by isolation and complete characterization of the products. Attempts have been made to establish the plausible pathway of the reference chemical transformations in our systems.

The platinum complexes, reported herein, represent a rare type of molecule<sup>13</sup> that features intense intramolecular charge transfer ( $\epsilon > 15000 \text{ M}^{-1} \text{ cm}^{-1}$ ) bands above 800 nm. The lowest energy charge transfer transitions in these complexes are primarily inter-ligand CT which may be tuned by changing the nature of the ligands. For example, the related compound *viz.* [Pt(bpy)(HN $\wedge$ SR)]<sup>+</sup> (bpy = 2,2'-bipyridine and HN $\wedge$ SR = 2-methylthioanilide) absorbs at a much shorter wavelength, near 540 nm.

## Result and discussion

Reactions of the molecular complex Pt(pap)Cl<sub>2</sub> [pap = 2-(phenylazo)pyridine] with three different S-substituted aminoth-

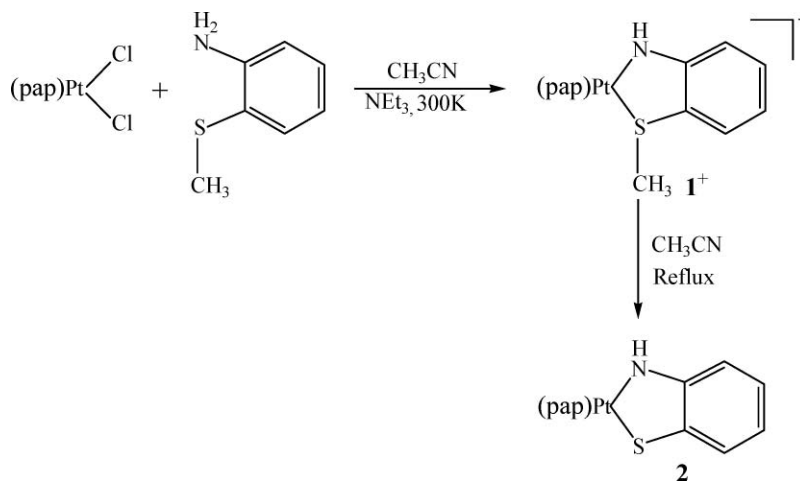
ioethers are studied in this work. X-ray structure along with the chemical reactions of the starting molecular compound, Pt(pap)Cl<sub>2</sub> were reported recently.<sup>3a,14</sup> Characteristic  $d\pi(\text{Pt})-\pi^*(\text{pap})$  interaction has been noted in this compound which is reflected in the elongation of the N–N and the shortening of the Pt–N(azo) distances.<sup>3a</sup>

### A. Chemical reaction of Pt(pap)Cl<sub>2</sub> and 2-methylthioaniline

The reaction of Pt(pap)Cl<sub>2</sub> and 2-methylthioaniline in the presence of NEt<sub>3</sub> (base) proceeds smoothly at room temperature producing the cationic mixed chelate, [Pt(pap)(HN $\wedge$ SMe)]Cl, ([1]Cl). The reaction involves substitution of two chlorides by the deprotonated 2-methylthioaniline. The above reaction in refluxing conditions, however, produced a molecular complex, [Pt(pap)(HN $\wedge$ S)] (2, H<sub>2</sub>N $\wedge$ SH = aminothiophenol) along with the above cationic complex indicating that the compound [1]Cl undergoes rupture of the S–C bond at a higher temperature. Accordingly, the pre-formed pure compound [1]Cl, when boiled in acetonitrile, produced compound 2 quantitatively in about two hours. The chemical reactions are summarized in Scheme 1.

Interestingly the above demethylation reaction [1]Cl  $\rightarrow$  2 was observed instantaneously even at a room temperature when the CH<sub>3</sub>CN solution of [1]Cl was reacted with an aqueous solution of KI. A similar transformation was also noted in the reaction between [1]Cl and excess of aqueous KBr or KCl, though the rate of reactions in the latter cases are considerably slower. These results signify that the coordinated sulfur atom in [1]Cl has induced significant electrophilic character on the adjacent alkyl carbon atom. This is not unexpected since a strong  $\pi$ -acidic nature of the co-ligand pap imparts electron deficiency at the coordinated S-atom in the reference compound making the S–C bond strongly polar. In this situation the S–C bond rupture may be envisaged primarily *via* heterolytic cleavage producing a methyl cation.

The electrospray ionization mass spectral data (ESI-MS) of the compounds [1]Cl and 2 has provided strong support in favor of the formulation of the complexes. Complex [1]Cl showed an intense peak at  $m/z$  516 amu along with a peak at 502 amu. The molecular complex 2, on the other hand, showed a single peak at  $m/z$  502 amu. The additional peak at  $m/z$  502 amu in the case of



Scheme 1

pure [1]Cl is due to the formation of **2** *via* demethylation under mass spectral conditions. The observed spectra of [1]Cl and [H2]<sup>+</sup> exactly corroborated with their simulated spectra (Fig. S1 and S2<sup>†</sup>).

The diamagnetic compound [1]Cl showed a resolved <sup>1</sup>H NMR spectrum in methanol-d<sub>4</sub>, however, a few peaks were broad. The protons of the neutral pap ligand resonate in the low field region ( $\delta$ , 9.54–7.69) with respect to the aromatic protons of 2-methylthioanilide ligand,  $\delta$ , 7.50–6.52. The NH proton and methyl proton resonances appeared at  $\delta$ , 4.57 and 2.20, respectively. The molecular compound **2** showed a highly resolved <sup>1</sup>H NMR spectrum in CDCl<sub>3</sub>. The <sup>1</sup>H NMR spectra of compounds [1]Cl and **2** are submitted as ESI (Fig. S3 and S4<sup>†</sup>). The most notable observation in the spectrum of compound **2** is the disappearance of the methyl resonance. In this complex the pyridyl and phenyl protons of the pap ligand resonate in the regions,  $\delta$ , 9.01–7.50 and  $\delta$ , 7.82–7.31, respectively. The aromatic protons of 2-methylthioanilide ligand experienced resonances in the relatively high field region,  $\delta$ , 7.45–6.64.

X-ray structure solution of the compound [1][OTf] (OTf = trifluoromethanesulfonate) reconfirms its formulation as well as its geometry. The central platinum atom in it is coordinated to a neutral pap and deprotonated 2-methylthioaniline ligands in a square planar geometry (Fig. 1). The complex as a whole is monocationic and the crystallographic asymmetric unit contains one OTf<sup>−</sup> as the counter anion. The Pt–N(azo) and Pt–N(py) distances are notably different, *viz.* 1.9645(19) and 2.020(2) Å, respectively. The shortness of the Pt–N(azo) bond in the compound may be attributed to  $d\pi-\pi\pi^*$  interaction between Pt(*t*<sub>2</sub>) and the low lying  $\pi^*$ (azo) molecular orbital of pap.

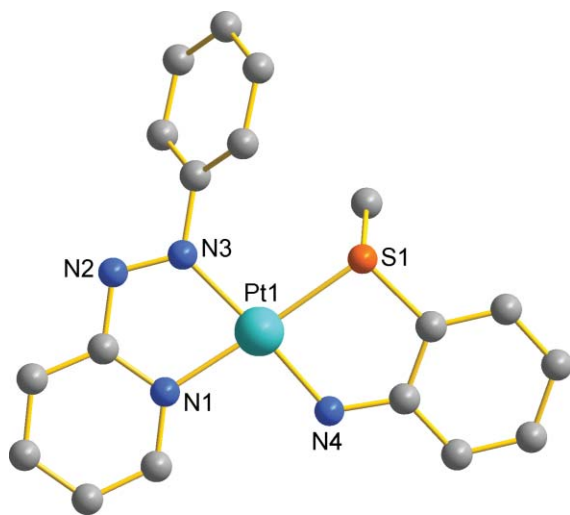


**Fig. 1** Molecular view of the compound, [Pt(pap)(HN<sup>SMe</sup>)<sup>+</sup> in [1][OTf].

Analysis of the X-ray structure of compound **2** (Fig. 2) has revealed the demethylation reaction as noted in Scheme 1. Consequently, the platinum atom in it is coordinated to a dianionic 2-amidothiophenolato ligand and a pap ligand. The bond lengths, Pt–N(py) and Pt–N(azo) are 2.045(3) and 1.968(5) Å respectively are different as in the cationic complex, [1][OTf]. Also, the C(ph)–S bond (1.738(7) Å) is shorter than that of a similar bond in the compound [1][OTf] (1.771(2) Å) signifying the anionic

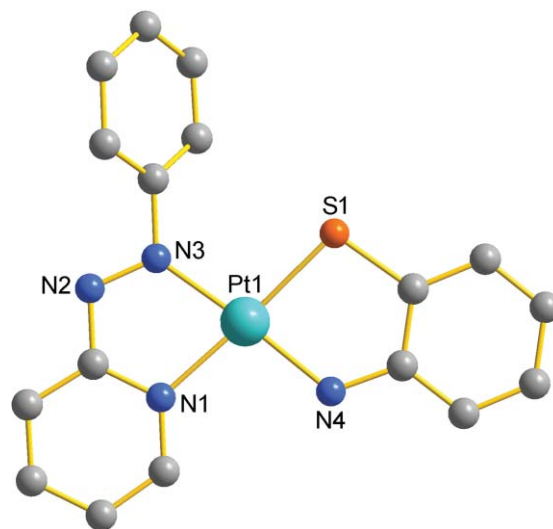


**Fig. 2** Molecular view of [Pt(pap)(HN<sup>S</sup>)], **2**.

nature of the deprotonated aminothiophenolate function. The C–N and C–S bond lengths in compound **2** are 1.364(8) and 1.738(7) Å respectively, which are in good accordance with the dianionic catecholate type coordination of the 2-amidothiophenolate ligand.<sup>15</sup>

## B. Reactions of Pt(pap)Cl<sub>2</sub> with 2-benzylthioaniline and 2-allylthioaniline

To have further insight into the above S–C bond cleavage reaction, two similar reactions of Pt(pap)Cl<sub>2</sub> with 2-benzylthioaniline and 2-allylthioaniline were planned. Since we have argued in favor of the heterolytic bond cleavage in the previous reaction (Scheme 1) and considering the unstable nature of the methyl cation, we now chose the benzyl and the allyl substituted thioethers since it is well established that both benzyl and allyl cations are far more stable than a methyl cation.

**(i) 2-benzylthioaniline.** In this case two products were isolated in nearly identical yield. One of these is the molecular compound **2** obtained due to debenzoylation and more interestingly, a second molecular compound **3** containing the deprotonated 2-(*N*-benzyl)aminothiophenol was also obtained in 35% yield. The formation of compound **3** from the above reaction involves debenzoylation of the thioether function and *N*-benzoylation of the coordinated amido nitrogen atom. This reaction was also followed in the presence of a radical scavenger, TEMPO (TEMPO = 2,2,6,6-tetramethylpiperidinoxy). Addition of TEMPO in a 1 : 1 molar proportion (with respect to 2-benzylthioaniline) to the reaction mixture, however, did not affect the yields or rate of reaction. Thus the possibility of the formation of benzyl radical *via* the homolytic S–C bond cleavage in these dealkylation reactions is excluded. We therefore propose here that heterolytic bond cleavage of the S–C bond is the primary step of the above reaction. The benzyl cation, thus formed, trapped by the coordinated amido nitrogen of the intermediate compound, **2** in alkaline conditions produced compound **3**.

In order to have theoretical support for the above chemical reaction, the net charge populations on the sulfur and nitrogen atoms (Fig. 3) of the 2-amidothiophenolate ligand in **2** were

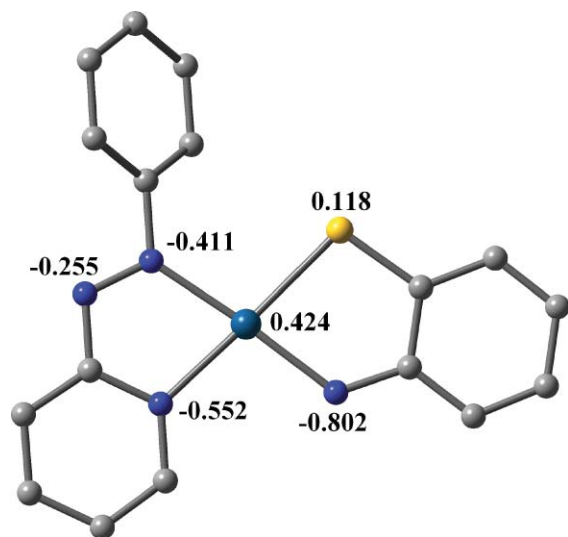


Fig. 3 Mulliken spin density view of **2**.

computed by the Gaussian03 program package. Clearly the nitrogen centre is more nucleophilic than the sulfur centre. This in turn correlates the observed N-alkylation reaction.

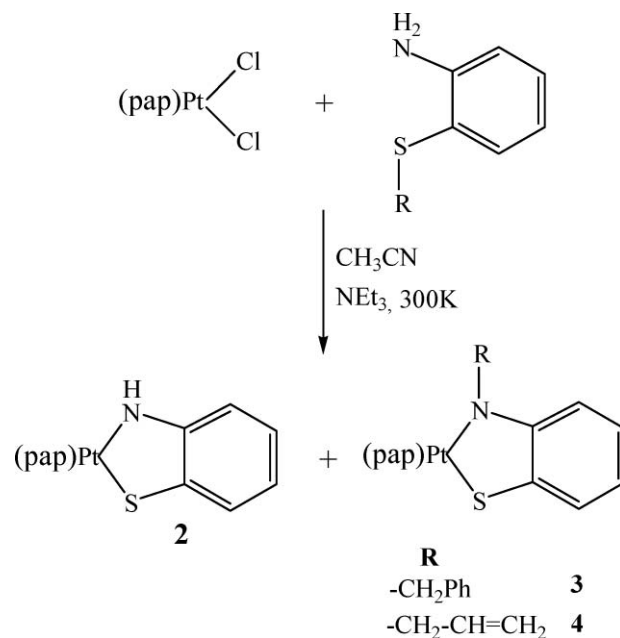
We also performed a similar reaction in the presence of an excess of KI. The reaction yielded the anticipated compound **2** as the only product. The formation of  $[\text{Ph-CH}_2]^+$  ( $m/z$ , 91 amu) in the reaction mixture was identified by the analysis of the ESI-MS spectrum of the reaction mixture. In this case strongly nucleophilic iodide anion traps the benzyl cation and prevents further attack of the coordinated anilido nitrogen centre. To prove it further, the pre-formed compound **2** was reacted with the salt, *N,N,N*-triethyl(*N*-benzyl)ammonium bromide, a potential source of the benzyl cation. The reaction yielded **3** confirming our proposition.

Compound **3** is a molecular compound and was characterized by ESI-MS,  $^1\text{H}$  NMR and elemental analyses. For example, the  $^1\text{H}$  NMR spectrum of **3** in  $\text{CDCl}_3$  is complex due to the presence of overlapping protons of the phenyl moieties of the two coordinated ligands. However, the four pyridyl proton resonances appeared in the lower field region ( $\delta$ , 8.56–7.47) were identified. The aliphatic methylene protons of the benzyl group resonate at  $\delta$ , 4.18. The ESI-MS and  $^1\text{H}$  NMR spectra of **3** are submitted as ESI (Fig. S5 and S6 $\dagger$ ).

**(ii) 2-Allylthioaniline.** The reaction of  $\text{Pt}(\text{pap})\text{Cl}_2$  and 2-allylthioaniline in acetonitrile proceeded similarly producing the deallylated compound, **2** and the N-allylated complex, **4**. The latter was characterized fully spectroscopically (Fig. S7 and S8 $\dagger$ ). Its single crystal structure determination by X-ray diffraction finally confirms the chemical transformations that are summarized in Scheme 2.

Analysis of the X-ray structures of compounds **3** and **4** has confirmed 1,4-migration of alkyl groups in the above reactions. The platinum atom in **3** is coordinated to a dianionic 2-(*N*-benzyl)amidothiophenolate ligand and a pap ligand. The Pt–N(azo) and Pt–N(py) distances are 1.969(8) and 2.055(8) Å respectively.

Similarly, the coordination sites of the Pt atom in compound **4** were satisfied by a dianionic 2-(*N*-allyl)amidothiophenolate ligand and a neutral pap ligand making the complex neutral. The Pt–



Scheme 2

N(azo) and Pt–N(py) distances are 1.961(8) Å and 2.071(8) Å respectively. The X-ray structures of the two compounds are shown in Fig. 4 and 5, respectively. Important bond parameters are collected in Table 1.

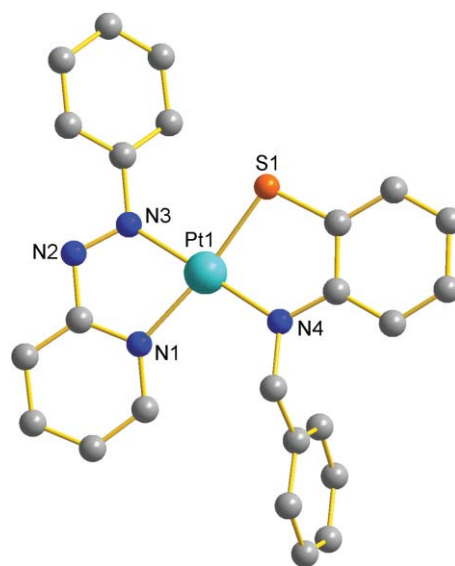


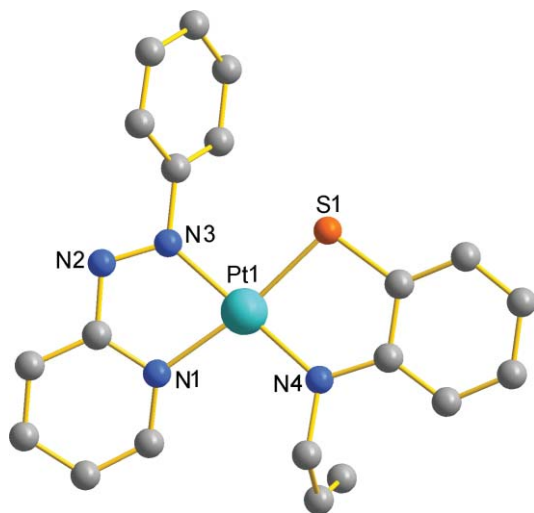
Fig. 4 Molecular view of  $[\text{Pt}(\text{pap})(\text{RN}^{\wedge}\text{S})]$ , **3**.

### C. Chemical reaction of $\text{Pt}(\text{bpy})\text{Cl}_2$ and 2-methylthioaniline

To examine the effect of the ancillary ligand, pap in the above S–C bond activation reactions, we planned a chemical reaction of  $\text{Pt}(\text{bpy})\text{Cl}_2$ <sup>16</sup> with 2-methylthioaniline under similar reaction conditions. The reaction produced a cationic mixed chelate,  $[\text{Pt}(\text{bpy})(\text{HN}^{\wedge}\text{SMe})\text{Cl}]$  (**5**) after 3 h stirring in acetonitrile in almost quantitative yield. The reaction involves simple substitution of two labile Cl atoms by the deprotonated 2-methylthioaniline.

**Table 1** Selected experimental and calculated bond lengths (Å) and angles (°) of [1][OTf], 2, 3 and [5][OTf]

Parameter	[1][OTf]		2		3	
	Exp.	Calc.	Exp.	Calc.	Exp.	Calc.
Pt(1)–S(1)	2.2783(7)	2.323	2.2707(16)	2.329	2.242(3)	2.313
Pt(1)–N(1)	2.020(2)	2.056	2.045(5)	2.061	2.055(8)	2.097
Pt(1)–N(3)	1.9645(19)	2.028	1.968(5)	2.004	1.969(8)	2.009
Pt(1)–N(4)	1.941(2)	1.981	1.988(5)	1.980	1.981(8)	2.023
N(2)–N(3)	1.292(3)	1.289	1.315(7)	1.313	1.295(11)	1.308
S(1)–C(17)	1.771(2)	1.777	1.738(7)	1.744	1.721(11)	1.738
N(4)–C(12)	1.376(3)	1.375	1.364(8)	1.366	1.366(13)	1.383
<b>S(1)–C(18)</b>	<b>1.817(3)</b>	<b>1.831</b>	<b>x</b>	<b>x</b>	<b>x</b>	<b>x</b>
S(1)–Pt(1)–N(3)	99.56(6)	101.8	99.79(15)	100.9	96.3(2)	97.1
S(1)–Pt(1)–N(4)	84.34(8)	82.38	83.54(15)	82.63	84.0(2)	83.4
N(1)–Pt(1)–N(3)	77.70(8)	77.04	77.61(19)	77.07	77.0(3)	76.2
N(1)–Pt(1)–N(4)	98.68(9)	98.69	99.03(19)	99.17	102.4(3)	103.1
Parameter	[5][OTf]					
	Exp.	Calc.				
Pt(1)–S(1)	2.259(9)	2.316				
Pt(1)–N(1)	2.036(3)	2.066				
Pt(1)–N(2)	2.025(3)	2.050				
Pt(1)–N(3)	1.981(3)	2.001				
S(1)–C(17)	1.814(4)	1.832				
S(1)–C(16)	1.774(4)	1.770				
N(3)–C(11)	1.355(5)	1.372				
S(1)–Pt(1)–N(2)	97.38(8)	99.54				
S(1)–Pt(1)–N(3)	84.43(10)	82.18				
N(1)–Pt(1)–N(2)	80.08(12)	78.99				
N(1)–Pt(1)–N(3)	98.12(13)	99.32				

**Fig. 5** Molecular view of [Pt(pap)(RN $\wedge$ S)], 4.

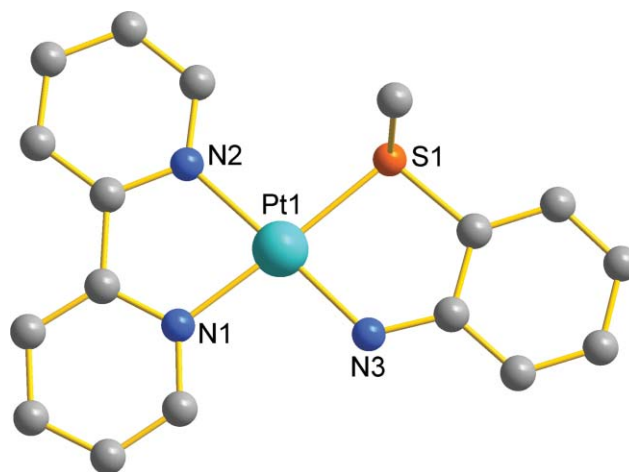
However, the cationic mixed chelate [5]Cl is chemically inert and does not undergo any change in refluxing conditions even in the presence of KI. This result is notable in the present context and confirms the active role of pap in the S–C bond activation process (*vide supra*).

To investigate the reasons for the different chemical behavior, we compared the relevant structural data of the two analogous compounds, [1][OTf] and [5][OTf]. Notably, the two Pt–N(py) bond lengths of the complex [5][OTf] are comparable with that of Pt–N(py) of pap in the compound [1][OTf] but are significantly longer than the Pt–N(azo) bond length. There has been very strong  $d\pi(\text{Pt})-p\pi^*(\text{azo})$  overlap in the pap containing complex. This effect has also been reflected in the HOMO–LUMO energy

gap in the compound [1][OTf] (1.75 eV) as compared to that in the compound [5][OTf] (1.92 eV). Such  $\pi$ -back donation is no doubt responsible for facilitating the S–C bond cleavage in all the above pap containing compounds.

The formulation of the complex, [5]Cl was also established by electrospray ionization mass spectrometry (ESI-MS) spectral data. The positive ion ESI mass spectrum of the complex was recorded in acetonitrile solvent and showed two peaks at  $m/z$  489 amu and 475 amu. The moderately intense peak at  $m/z$  475 amu in [5]Cl is due to the formation of the demethylated compound indicating S–C bond rupture in mass spectral conditions. The observed isotropic distributions of the above two peaks exactly corroborated with their simulated patterns (Fig. S9 $\dagger$ ). The diamagnetic compound [5]Cl showed resolved  $^1\text{H}$  NMR spectrum in methanol- $d_4$ . The protons of the neutral bpy ligand resonate in the low field region ( $\delta$ , 9.17–7.70) with respect to the aromatic protons of 2-methylthioanilide ligand at  $\delta$ , 7.16–6.37. The NH proton and methyl proton resonances appeared at  $\delta$ , 4.90 and 2.84, respectively. The spectrum of the compound [5]Cl is submitted as ESI (Fig. S10 $\dagger$ ).

The X-ray structure of the salt [5][OTf] (OTf = trifluoromethanesulfonate) was solved, which also confirms its formulation as well as geometry. The central platinum atom in the compound is coordinated to a neutral bpy and a deprotonated 2-methylthioaniline ligand in a square planar geometry (Fig. 6). The complex as a whole is monocationic and the crystallographic asymmetric unit contains one OTf $^-$  as the counter anion and water molecules as solvate. The average Pt–N(bpy) and Pt–N(anilido) distances are 2.030(3) and 1.981(3) Å respectively.

**Fig. 6** Molecular view of [Pt(bpy)(HN $\wedge$ SMe)] $^+$  in [5][OTf].

#### D. UV-vis spectra and DFT

All the pap-containing compounds exhibited low-energy absorption spectra with broad allowed band(s) near 800 nm and above (Table 2, Fig. 7). For example, the molecular compounds, 2, 3 and 4 showed a transition near 800 nm which was associated with a shoulder near 700 nm. The low energy part of the spectra of the cationic complexes, [1][OTf] and [5][OTf] on the other hand, consisted of a single intense transition. The assignment of these transitions was guided by the results from DFT calculations. The molecular structures of all the complexes were fully optimized

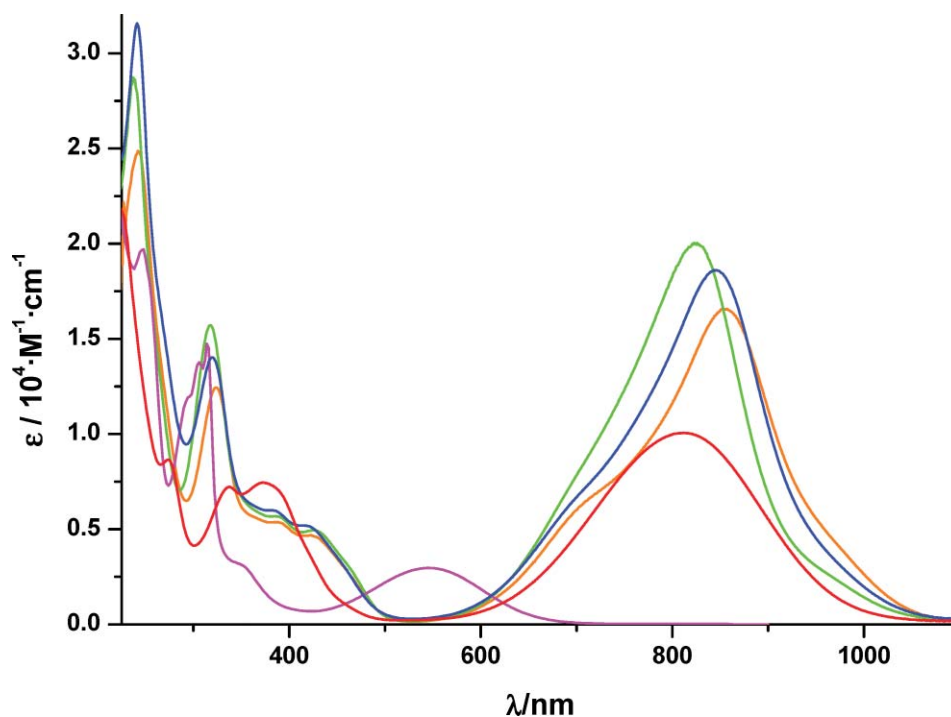


Fig. 7 UV-vis-NIR absorption spectra of the compounds, [1][OTf] (red), 2 (green), 3 (orange), 4 (blue) and [5][OTf] (pink) in  $10^{-4}$  M acetonitrile solution.

Table 2 UV-vis-NIR spectral data<sup>a</sup> in  $\text{CH}_3\text{CN}$  solvent of all reported compounds

Compound	$\lambda_{\text{max}}$ <sup>a</sup> ( $\epsilon$ )
[1][OTf]	815(10040), 375(7445), 340(7200), 275(8520)
2	825(19960), 700 <sup>b</sup> , 425(5020), 390(5755), 315(15650), 240(28680),
3	855(16575), 700 <sup>b</sup> , 425(4560), 390(5410), 325(12460), 240(24850)
4	846(18581), 700 <sup>b</sup> , 422(5167), 384(6027), 319(14239), 240(31525)
[5][OTf]	545(2984), 352(3077), 314(14564), 246(19704), 216(23274)

<sup>a</sup> Wavelength in nm, molar extinction coefficients in  $\text{M}^{-1} \text{cm}^{-1}$ . <sup>b</sup> Shoulder.

at the B3LYP level of theory. The calculated bond lengths and angles compared well with the crystallographically established metrical parameters (see ESI, Tables S1–S4†). These two sets of numbers are in good agreement with as the bond lengths and angles are predicted within 2 pm and  $1\text{--}4^\circ$  of the experimental values, respectively. However, the Pt–S and Pt–N bond lengths are overestimated (Pt–S,  $\sim 0.05\text{--}0.06 \text{ \AA}$ , Pt–N(azo),  $\sim 0.035\text{--}0.06 \text{ \AA}$ , Pt–N(pyridyl),  $\sim 0.015\text{--}0.04 \text{ \AA}$  and Pt–N(amine),  $\sim 0.01\text{--}0.04 \text{ \AA}$ ). The azo N–N bond length is slightly underestimated by about  $0.002\text{--}0.020 \text{ \AA}$ . This difference arises most likely from crystallographic packing and such interactions are not modeled in the calculations.

Analyses of the MOs of the complexes ([1][OTf], 2, 3 and [5][OTf]) reveal that the highest occupied MOs are centered on the 2-amidothioether or 2-amidothiophenolate ligands. The lowest unoccupied MOs are also of ligand character and localized over the  $\pi^*$  orbital of the pap or the bpy ligand. The electron density distribution of the HOMO, HOMO-1 and LUMO and the relative

contributions of metal and ligand orbitals to the corresponding MOs are submitted as ESI (Fig. S11–S14, Tables S5–S8†).

The calculated excitation energies using TD-DFT for all these complexes are collected in Tables S9–S12.† The low energy bands for compounds [1][OTf], 2 and 3 appeared in the range, 850–800 nm. The experimental transitions compared well with the calculated values for HOMO/HOMO-1  $\rightarrow$  LUMO transitions. This band in the bpy analogue, [5][OTf] shifted to a much higher frequency, at 545 nm. The lowest energy transition in all the cases can be described as interligand charge transfer. In the complex, [5][OTf] the acceptor orbitals lie at higher energies resulting in a significant blue shift of the interligand transition. The mid-intensity peak in [1][OTf] with a transition maximum close to 382 nm may be assigned to the HOMO-2  $\rightarrow$  LUMO transition. Similarly compounds 2 and 3 exhibited low intensity peaks near 425 nm which are assigned to HOMO-2  $\rightarrow$  LUMO and HOMO-3  $\rightarrow$  LUMO transitions. Several other transitions were observed between 400 to 300 nm.

### E. Cyclic voltammetry and EPR

Redox properties of all the reference complexes were studied by cyclic voltammetry (CV) in acetonitrile solvent (0.1 M TEAP), with a platinum working electrode. The potentials are referenced to the saturated Ag/AgCl electrode and the data are collected in Table 3. Segmented voltammograms (cathodic sweep) of the two representative compounds are displayed in Fig. 8 and their full range (+1.6 to  $-1.6$  V) voltammograms are submitted as ESI (Fig. S15†).

The complex [1][OTf] displayed four electrochemical responses at 0.94, 0.48,  $-0.21$  and  $-0.94$  V. The two responses at cathodic potentials are reversible while the oxidative responses are irreversible. The nature of the voltammograms of the

**Table 3** Cyclic voltammetric data<sup>a</sup>

Compound	Reduction $-E_{2/1}$ <sup>b</sup> V ( $\Delta E_p$ , mV)	Oxidation $E_{2/1}$ <sup>b</sup> V ( $\Delta E_p$ , mV)
[1][OTf]	-0.21(90), -0.94(90)	0.48 <sup>c</sup> , 0.94 <sup>c</sup>
<b>2</b>	-0.68(80), -1.35(80)	0.50 <sup>c</sup>
<b>3</b>	-0.71(90), -1.38(86)	0.54 <sup>c</sup>
<b>4</b>	-0.68(80), -1.35(82)	0.54 <sup>c</sup>

<sup>a</sup> In acetonitrile solution supporting electrolyte Et<sub>4</sub>NClO<sub>4</sub>, reference electrode Ag/AgCl. <sup>b</sup>  $E_{1/2} = 0.5(E_{pa} + E_{pc})$  where  $E_{pa}$  and  $E_{pc}$  are anodic and cathodic peak potentials respectively,  $\Delta E_p = E_{pa} - E_{pc}$ , scan rate 50 mV s<sup>-1</sup>. <sup>c</sup> Irreversible.

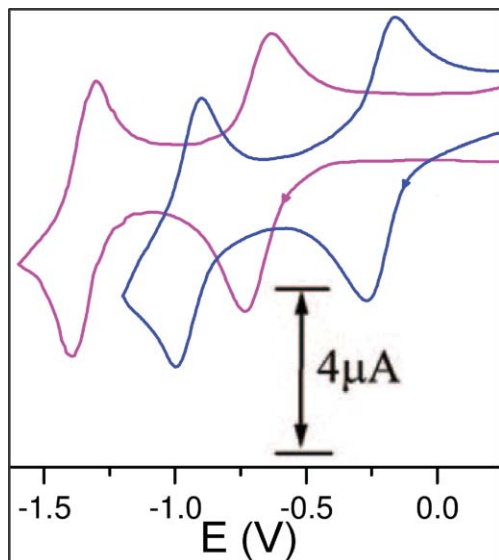


**Fig. 8** Cyclic voltammograms of the compound [1][OTf] (blue) and **2** (pink) in CH<sub>3</sub>CN/0.1 M Et<sub>4</sub>NClO<sub>4</sub>.

S-dealkylated/N-alkylated compounds **2**, **3** and **4** is nearly identical. They exhibit one irreversible anodic response between 0.50 and 0.54 V and two reversible cathodic responses near -0.60 and -1.30 V. The one-electron redox response has been confirmed by comparison of the current height with the redox response of the ferrocene/ferrocenium couple under identical experimental conditions (for irreversible waves) and by constant-potential electrolysis for the reversible waves. Irreversible responses at the anodic potentials can be assigned to the oxidation of the donor ligands, 2-amidothiophenolate or 2-amidothioether while the cathodic waves formally correspond to the reduction of the azo chromophore of the pap ligand. These results are fully supported by the FMOs which clearly indicate that the LUMO and HOMO of the complexes [1][OTf], **2** and **3** are primarily ligand centered. The irreversible nature of the oxidative responses may be attributed to rapid ligand substitution and complex degradation upon electron transfer.

To have an insight into the nature of the electronic levels associated with the reversible redox processes, electrogenerated complexes were studied by EPR and UV-vis-NIR spectroelectrochemistry in CH<sub>3</sub>CN/0.1 M Et<sub>4</sub>NClO<sub>4</sub> at 120 K. The one electron reduced complex [1], generated by exhaustive electrolysis of [1][OTf] at -0.40 V, showed an EPR signal with strong hyperfine coupling<sup>13b</sup> constants of 7.3 and 2.9 mT (for <sup>195</sup>Pt,  $I = \frac{1}{2}$ , natural abundance = 33%) at  $g = 2.001$  confirming some metal

participation to the SOMO, the second electron reduced species is however EPR silent. Similarly, the one electron reduced complexes **2**<sup>-</sup>, **3**<sup>-</sup> and **4**<sup>-</sup> showed an EPR signal with  $g$  values of 2.005, 2.008 and 2.005 with metal hyperfine coupling constants of 12.6 and 6.4; 11.9 and 4.9; 12.4 mT respectively. EPR spectra of all the above one electron reduced complexes are submitted as ESI (Fig. S16<sup>†</sup>). Notably the color of the solutions of the above complexes faded considerably upon reduction. This is not unexpected since the acceptor character of the pap ligand diminishes upon reduction resulting in the disappearance of the above interligand transitions.

## F. Conclusion

In this work we have disclosed unusual examples of 1,4-migration of alkyl groups associated with simultaneous S-C bond cleavage and N-C bond formation in the platinum complexes of 2-amidothioether ligands. Design of the chemical reactions with chosen substrates has been used to understand the course of these reactions. The reference chemical reactions are promoted by the presence of the coligand, 2-(phenylazo)pyridine. Strong  $d\pi(\text{Pt})-\pi^*(\text{azo})$  interactions in these complexes activate the S-C bond, which is the driving force for the above transformations. For comparison, the 2,2'-bipyridine analogue failed to promote the above organic transformations. The products of the reactions are fully characterized using spectral studies and X-ray structure determination. The complex molecules containing pap showed allowed charge transfer in the near IR-region (>800 nm), and are assigned to intramolecular interligand transitions. The low energy transition in the bpy-analogue shifts blue and appear in the visible region (near 545 nm). A parallel trend in the reduction potentials and the energies of LUMOs in the pap- and bpy- complexes are also noted.

## Experimental section

### Materials

The starting Pt-salt, K<sub>2</sub>PtCl<sub>4</sub> was collected from Arora-Matthey, Kolkata. The ligand 2-methylthioaniline was purchased from Sigma-Aldrich. The three other ligands, 2-benzylthioaniline, 2-allylthioaniline and pap [2-(phenylazo)pyridine] were prepared<sup>17,18</sup> as before. The compound Pt(pap)Cl<sub>2</sub><sup>3a,14</sup> and tetraethylammonium perchlorate (TEAP)<sup>19</sup> were prepared and crystallized following published procedures. **Caution!** perchlorate salts have to be handled with care and appropriate safety precautions. Solvents and chemicals used for syntheses were of analytical grade and used as received.

### Instrumentation

UV-vis-NIR absorption spectra were recorded either on a Perkin-Elmer Lambda 950 UV/vis spectrophotometer or on a J&M TIDAS instrument. The IR spectra were recorded with a Perkin-Elmer 783 spectrophotometer. Cyclic voltammetry was carried out in 0.1 M TEAP solutions using a three-electrode configuration (platinum working electrode, Pt counter electrode, Ag/AgCl reference electrode) and a PC-controlled PAR model 273A electrochemistry system. The  $E_{1/2}$  for the ferrocenium-ferrocene couple under our experimental conditions was 0.39 V. EPR spectra in the X band were recorded with a JEOL JES-FA200 spectrometer. A

Perkin-Elmer 240C elemental analyzer was used to collect micro analytical data (C, H, N).  $^1\text{H}$  NMR spectra were taken on a Bruker Avance DPX 300 spectrometer, and  $\text{SiMe}_4$  was used as the internal standard. ESI mass spectra were recorded on a micro mass Q-TOF mass spectrometer (serial No. YA 263). A Perkin-Elmer 240C elemental analyzer was used to collect microanalytical data (C, H, N).

## Syntheses

Syntheses of the complexes were carried out by the reaction of neutral  $\text{Pt}(\text{pap})\text{Cl}_2$  and  $\text{Pt}(\text{bpy})\text{Cl}_2$  with aminothioether in the presence of  $\text{NEt}_3$  in acetonitrile solvent.

### a. Chemical reactions of $[\text{Pt}(\text{pap})\text{Cl}_2]$ with 2-alkylthioanilines

**(i) 2-methylthioaniline.** To a solution of 50 mg (0.11 mmol)  $\text{Pt}(\text{pap})\text{Cl}_2$  in 30 ml of acetonitrile, 16 mg (0.11 mmol) 2-methylthioaniline ( $\text{H}_2\text{N}\wedge\text{SMe}$ ) was added followed by the addition of 2 drops of  $\text{NEt}_3$ . The color of the solution changed from dark red to intense green instantaneously. The mixture was then stirred for 30 min at room temperature. The crude compound obtained after evaporation of the solvent was purified on a preparative alumina TLC plate. Toluene–methanol solvent mixture was used as the eluent. The compound  $[\text{Pt}(\text{pap})(\text{HN}\wedge\text{SMe})]\text{Cl}$ , (**[1]Cl**) was separated on a TLC plate as a major green band. The residue obtained by solvent evaporation was crystallized from methanol containing excess of sodium trifluoromethanesulfonate ( $\text{NaOTf}$ ). Highly crystalline **[1][OTf]** was obtained in 90% yield. Anal. Calcd for  $\text{C}_{19}\text{H}_{17}\text{N}_4\text{PtS}_2\text{F}_3\text{O}_3$ : C, 34.28; H, 2.56; N, 8.42. Found: C, 34.23; H, 2.51; N, 8.49. IR (KBr disk,  $\text{cm}^{-1}$ ): 1600 (C=N), 1319 (N=N). ESI-MS:  $m/z$  516 amu, **[1]**<sup>+</sup>.

**(ii) Conversion of  $[\text{Pt}(\text{pap})(\text{HN}\wedge\text{SMe})]\text{Cl}$ , (**[1]Cl**) to  $[\text{Pt}(\text{pap})(\text{HN}\wedge\text{S})]$ , **2** ( $\text{HN}\wedge\text{S} = 2\text{-amidothiophenolate}$ ).** The compound **2** was obtained almost quantitatively by boiling an acetonitrile solution of the compound **[1]Cl** or by treating the same with aqueous KI solution at room temperature. Anal. Calcd for  $\text{C}_{17}\text{H}_{14}\text{N}_4\text{PtS}$ : C, 40.72; H, 2.80; N, 11.20. Found: C, 40.78; H, 3.2; N, 11.14. IR (KBr disk,  $\text{cm}^{-1}$ ): 1600 (C=N), 1292 (N=N). ESI-MS:  $m/z$  502 amu, **[H2]**<sup>+</sup>.

**(iii) 2-Benzylthioaniline.** A solution of 50 mg (0.11 mmol)  $\text{Pt}(\text{pap})\text{Cl}_2$  in 30 ml acetonitrile was reacted with 24 mg (0.11 mmol) 2-benzylthioaniline in the presence of 2 drops of  $\text{NEt}_3$ . The color of the solution immediately changed from dark red to intense green at room temperature. The mixture was stirred for 1 h. The crude mass obtained by evaporation of the solvent was dissolved in a minimum volume of dichloromethane and loaded on to a preparative silica-gel TLC plate for purification. Toluene was used as the eluent. Two green bands were obtained. The first green zone upon evaporation yielded the compound **2**. The second green zone produced a new compound  $[\text{Pt}(\text{pap})(\text{RN}\wedge\text{S})]$ , **3** ( $\text{RN}\wedge\text{S} = 2\text{-}(N\text{-benzyl})\text{amidothiophenolate}$ ). The solvent was evaporated and the residue was crystallized by slow evaporation of a dichloromethane–methanol solution mixture. Yield: 35%. ESI-MS,  $m/z$ : 593 amu **[H3]**<sup>+</sup>. Anal. Calcd for  $\text{C}_{24}\text{H}_{20}\text{N}_4\text{PtS}$ : C, 48.65; H, 3.38; N, 9.46. Found: C, 48.61; H, 3.46; N, 9.38. IR (KBr disk,  $\text{cm}^{-1}$ ): 1599 (C=N), 1296 (N=N).

**(iv) 2-Allylthioaniline.** Another similar reaction of  $\text{Pt}(\text{pap})\text{Cl}_2$  with 2-allylthioaniline yielded the compound  $[\text{Pt}(\text{pap})(\text{RN}\wedge\text{S})]$ , **4** ( $\text{RN}\wedge\text{S} = 2\text{-}(N\text{-allyl})\text{amidothiophenolate}$ ) along with compound **2**. Reaction conditions as well as purification of the products are similar to that described above in section (iii). The yield and characterization data of the compound **4** are as follows.

Yield: 35%. ESI-MS,  $m/z$ : 543 amu **[H4]**<sup>+</sup>. Anal. Calcd for  $\text{C}_{20}\text{H}_{19}\text{N}_4\text{PtS}$ : C, 44.28; H, 3.50; N, 10.33. Found: C, 44.24; H, 3.45; N, 10.27. IR (KBr disk,  $\text{cm}^{-1}$ ): 1599 (C=N), 1294 (N=N).

### b. Chemical reaction of $[\text{Pt}(\text{bpy})\text{Cl}_2]$ with 2-methylthioaniline

A mixture of 47 mg (0.11 mmol)  $\text{Pt}(\text{bpy})\text{Cl}_2$  and 16 mg (0.11 mmol) 2-methylthioaniline ( $\text{H}_2\text{N}\wedge\text{SMe}$ ) in 30 ml of acetonitrile in the presence of 2 drops of  $\text{NEt}_3$  was stirred for 3 h at room temperature. The yellow solution became violet during this period. The crude mass obtained by evaporation of the solvent was dissolved in a minimum volume of methanol and was loaded on to a preparative alumina TLC plate for purification. Chloroform–methanol solvent mixture was used as the eluent. A broad violet zone was collected. Evaporation of the solvent yielded the compound  $[\text{Pt}(\text{pap})(\text{HN}\wedge\text{SMe})]\text{Cl}$ , (**[5]Cl**). It was finally crystallized from methanol containing an excess of sodium trifluoromethanesulfonate ( $\text{NaOTf}$ ). A highly crystalline compound, **[5][OTf]** was obtained in 90% yield. Anal. Calcd for  $\text{C}_{18}\text{H}_{16}\text{N}_3\text{PtS}_2\text{F}_3\text{O}_3$ : C, 33.85; H, 2.51; N, 6.58. Found: C, 33.79; H, 2.55; N, 6.63. IR (KBr disk,  $\text{cm}^{-1}$ ): 1608 (C=N), 1319 (N=N). ESI-MS:  $m/z$  489 amu, **[5]**<sup>+</sup>.

## Computational details

Full geometry optimizations were carried out using the density functional theory method at the (R)B3LYP level.<sup>20</sup> All elements except platinum were assigned using the 6-31G(d) basis set. The SDD basis set with effective core potential was employed for the platinum atom.<sup>21</sup> The vibrational frequency calculations were performed to ensure that the optimized geometries represented the local minima and there were only positive eigen values. All calculations were performed with the Gaussian03 program package.<sup>22</sup> Natural bond orbital analyses were performed using the NBO 3.1 module of Gaussian03.<sup>23</sup> Vertical electronic excitations based on B3LYP optimized geometries were computed using the time-dependent density functional theory (TD-DFT) formalism<sup>24</sup> in methanol using a conductor-like polarizable continuum model (CPCM).<sup>25</sup> GaussSum<sup>26</sup> was used to calculate the fractional contributions of various groups to each molecular orbital.

## Crystallography

Crystallographic data for the compounds **[1][OTf]**, **2**, **3**, **4** and **[5][OTf]** are collected in Table 4 and their ORTEP and atom numbering scheme are submitted as ESI (Fig. S17–S21†). Suitable X-ray quality crystals of the cationic compounds were obtained from slow evaporation of their methanolic solutions. Suitable crystals of the molecular compounds on the other hand were obtained by slow evaporation of dichloromethane–methanol solutions of the compounds. All data were collected on a Bruker SMART APEX diffractometer, equipped with graphite monochromated

**Table 4** Crystallographic data for [1][OTf], 2, 3, 4 and [5][OTf]

Parameter	[1][OTf]	2	3	4	[5][OTf]
Empirical formula	C <sub>16</sub> H <sub>17</sub> N <sub>4</sub> PtS <sub>2</sub> O <sub>3</sub> F <sub>3</sub>	C <sub>17</sub> H <sub>14</sub> N <sub>4</sub> PtS	C <sub>24</sub> H <sub>20</sub> N <sub>4</sub> PtS	C <sub>20</sub> H <sub>18</sub> N <sub>4</sub> PtS	C <sub>36</sub> H <sub>32</sub> N <sub>3</sub> PtS <sub>4</sub> F <sub>6</sub> O <sub>7</sub>
Formula weight	665.59	501.47	592.60	541.53	654.55
Crystal System	Triclinic	Monoclinic	Monoclinic	Triclinic	Orthorhombic
Space group	$P\bar{1}$	$P2_1/n$	$P2_1/c$	$P\bar{1}$	$Pbcn$
<i>a</i> /Å	9.4100(5)	6.8962(6)	11.4495(8)	12.476(3)	9.2882(3)
<i>b</i> /Å	10.5974(6)	22.833(2)	19.8920(13)	18.2405(14)	20.4170(5)
<i>c</i> /Å	11.4765(6)	10.0507(9)	27.4519(19)	18.3912(14)	21.1399(6)
$\alpha$ (°)	84.0250(10)	90	90	118.647(10)	90.00
$\beta$ (°)	78.3860(10)	92.612(4)	98.806(2)	97.985(10)	90.00
$\gamma$ (°)	72.4940(10)	90	90	93.079(10)	90.00
<i>V</i> /Å <sup>3</sup>	1067.94(10)	1581.0(2)	6178.6(7)	3602.3(10)	4008.9(2)
<i>Z</i>	2	4	12	8	8
<i>D</i> <sub>calcd</sub> /g cm <sup>-3</sup>	2.070	2.107	1.908	1.997	2.142
Cryst dimens/mm <sup>3</sup>	0.07 × 0.17 × 0.20	0.07 × 0.15 × 0.24	0.08 × 0.16 × 0.18	0.10 × 0.14 × 0.25	0.10 × 0.10 × 0.10
$\theta$ range for data collection (°)	1.8–25.0	1.8–29.5	1.3–27.6	1.3–25.0	1.9–29.7
GOF on <i>F</i> <sup>2</sup>	1.02	1.02	1.04	1.02	1.01
Reflections collected	12737	25683	41931	26097	49301
Unique reflection	3765	4350	13010	12595	5633
Final <i>R</i> indices [ <i>I</i> > 2 $\sigma$ ( <i>I</i> )]	<i>R</i> <sub>1</sub> = 0.0167 <i>wR</i> <sub>2</sub> = 0.0418	<i>R</i> <sub>1</sub> = 0.0398 <i>wR</i> <sub>2</sub> = 0.0888	<i>R</i> <sub>1</sub> = 0.0381 <i>wR</i> <sub>2</sub> = 0.0798	<i>R</i> <sub>1</sub> = 0.0291 <i>wR</i> <sub>2</sub> = 0.0756	<i>R</i> <sub>1</sub> = 0.0285 <i>wR</i> <sub>2</sub> = 0.0593
<i>T</i> /K	293	293	293	293	293

Mo-K $\alpha$  radiation ( $\lambda = 0.71073$  Å), and were corrected for Lorentz-polarization effects. [1][OTf]: A total of 12737 reflections were collected, of which 3765 were unique ( $R_{\text{int}} = 0.022$ ), satisfying the ( $I > 2\sigma(I)$ ) criterion, and were used in subsequent analysis. 2: A total of 25683 reflections were collected, of which 4350 were unique ( $R_{\text{int}} = 0.085$ ). 3: A total of 41931 reflections were collected, of which 13010 were unique ( $R_{\text{int}} = 0.097$ ). 4: A total of 26097 reflections were collected, of which 12595 were unique ( $R_{\text{int}} = 0.031$ ). [5][OTf]: A total of 49301 reflections were collected, of which 5633 were unique ( $R_{\text{int}} = 0.074$ ).

The structures were solved by employing the SHELXS-97 program package<sup>27a</sup> and were refined by full-matrix least-squares based on *F*<sup>2</sup> (SHELXL-97).<sup>27b</sup> All hydrogen atoms were added in calculated positions.

### EPR spectral studies

The one electron reduced complexes [1], 2<sup>-</sup>, 3<sup>-</sup> and 4<sup>-</sup>, generated by exhaustive electrolysis of [1][OTf] at -0.40 V in CH<sub>3</sub>CN/0.1 M Et<sub>4</sub>NClO<sub>4</sub>, were immediately dipped into liquid nitrogen and the resulting frozen solutions were used for the EPR measurements at 120 K. The applied potential for the complexes 2, 3, and 4 is -0.80 V.

### Acknowledgements

Financial support received from the Council of Scientific and Industrial Research (CSIR), New Delhi (Project 01/2358/09/EMR-II) is gratefully acknowledged. Crystallography was performed at the DST-funded National Single Crystal Diffractometer Facility at the Department of Inorganic Chemistry, IACS. S.M. thanks the Council of Scientific and Industrial Research for her fellowship.

### References

- (a) C. Makedonas, A. C. Mitsopoulou, J. F. Lahoz and I. A. Balana, *Inorg. Chem.*, 2003, **42**, 8853; (b) S. Huertas, M. Hissler, J. E. McGarrah, R. J. Lachicotte and R. Eisenberg, *Inorg. Chem.*, 2001, **40**, 1183; (c) M. Hissler, I. E. McGarrah, W. B. Connick, D. K. Geiger, S. D. Cummings and R. Eisenberg, *Coord. Chem. Rev.*, 2000, **208**, 115; (d) W. B. Connick, D. Geiger and R. Eisenberg, *Inorg. Chem.*, 1999, **38**, 3264.
- (a) E. Shikhova, E. O. Danilov, S. Kinayyigit, I. E. Pomestchenko, A. D. Tregubov, F. Camerel, P. Retailleau, R. Ziessel and F. N. Castellano, *Inorg. Chem.*, 2007, **46**, 3038; (b) I. Eryazici, C. N. Moorefield and G. R. Newkome, *Chem. Rev.*, 2008, **108**, 1834; (c) X.-J. Liu, J.-K. Feng, J. Meng, Q.-J. Pan, A.-M. Ren, X. Zhou and H.-X. Zhang, *Eur. J. Inorg. Chem.*, 2005, 1856; (d) X. Zhou, H.-X. Zhang, Q.-J. Pan, B.-H. Xia and A.-C. Tang, *J. Phys. Chem. A*, 2005, **109**, 8809; (e) F. Hua, S. Kinayyigit, J. R. Cable and F. N. Castellano, *Inorg. Chem.*, 2006, **45**, 4304; (f) A. M. E. Geary, J. L. Yellowlees, A. L. Jack, D. H. I. Oswald, S. Parsons, N. Hirata, R. J. Durrant and N. Robertson, *Inorg. Chem.*, 2005, **44**, 242.
- See, for example: (a) M. Panda, S. Das, G. Mostafa, A. Castiñeiras and S. Goswami, *Dalton Trans.*, 2005, 1249; (b) M. Panda, C. Das, G.-H. Lee, S.-M. Peng and S. Goswami, *Dalton Trans.*, 2004, 2655; (c) A. K. Deb, M. Kakoti and S. Goswami, *J. Chem. Soc., Dalton Trans.*, 1991, 3249; (d) A. K. Deb, S. Choudhury and S. Goswami, *Polyhedron*, 1990, **9**, 2251; (e) M. N. Ackermann, C. R. Barton, C. J. Deodene, E. M. Specht, S. C. Keill, W. E. Schreiber and H. Kim, *Inorg. Chem.*, 1989, **28**, 397; (f) S. Wolfgang, T. C. Strekas, H. D. Gafney, A. R. Krause and K. Krause, *Inorg. Chem.*, 1984, **23**, 2650; (g) S. Goswami, A. R. Chakravarty and A. Chakravorty, *Inorg. Chem.*, 1981, **20**, 2246.
- (a) M. K. C. Chan, C.-H. Tao, H.-L. Tam, N. Zhu, W.-W. V. Yam and K.-W. Cheah, *Inorg. Chem.*, 2009, **48**, 2855; (b) N. J. Wheate, R. I. Taleb, A. M. Krause-Heuer, R. L. Cook, S. Wang, V. J. Higgins and J. R. Aldrich-Wright, *Dalton Trans.*, 2007, 5055; (c) J. R. Mishur, C. Zheng, M. Thomas, M. T. Gilbert, N. Rathindra and N. R. Bose, *Inorg. Chem.*, 2008, **47**, 7972; (d) H.-S. Lo, S.-K. Yip, K. M.-C. Wong, N. Zhu and V. W.-W. Yam, *Organometallics*, 2006, **25**, 3537; (e) K. M.-C. Wong, W.-S. Tang, X.-X. Lu, N. Zhu and V. W.-W. Yam, *Inorg. Chem.*, 2005, **44**, 1492; (f) C. Das, A. Saha, C.-H. Hung, G.-H. Lee, S.-M. Peng and S. Goswami, *Inorg. Chem.*, 2003, **42**, 198.
- (a) S. Chatterjee, P. Singh, J. Fiedler, R. Baková, S. Zális, W. Kaim and S. Goswami, *Dalton Trans.*, 2009, 7778; (b) K. N. Mitra, S.-M. Peng and S. Goswami, *Chem. Commun.*, 1998, 1685; (c) K. N. Mitra, S. Choudhury, A. Castiñeiras and S. Goswami, *J. Chem. Soc., Dalton Trans.*, 1998, 2901; (d) K. N. Mitra, P. Majumdar, S.-M. Peng, A. Castiñeiras and S. Goswami, *Chem. Commun.*, 1997, 1267; (e) K. N. Mitra and S. Goswami, *Chem. Commun.*, 1997, 49; (f) A. Saha, C. Das, K. N. Mitra, S.-M. Peng, G. H. Lee and S. Goswami, *Polyhedron*, 2002, **21**, 97; (g) K. N. Mitra and S. Goswami, *Inorg. Chem.*, 1997, **36**, 1322.
- (a) N. Roy, S. Stephen, E. Bill, T. Weyhermüller and K. Wieghardt, *Inorg. Chem.*, 2008, **47**, 10911; (b) D. Herebian, E. Bothe, E. Bill, T. Weyhermüller and K. Wieghardt, *J. Am. Chem. Soc.*, 2001, **123**, 10012.
- M. D. Roundhill, *Inorg. Chem.*, 1980, **19**, 557.

- 8 S. Chatterjee and S. Goswami, unpublished results.
- 9 (a) P. Chaudhuri, M. Hess, J. Müller, K. Hildenbrand, E. Bill, T. Weyhermüller and K. Wieghardt, *J. Am. Chem. Soc.*, 1999, **121**, 9599; (b) P. Chaudhuri, M. Hess, U. Flörke and K. Wieghardt, *Angew. Chem., Int. Ed.*, 1998, **37**, 2217; (c) M. R. Wachter, P. M. Montague-Smith and P. B. Branchaud, *J. Am. Chem. Soc.*, 1997, **119**, 7743.
- 10 M. Shibue, M. Hirotsu, T. Nishioka and I. Kinoshita, *Organometallics*, 2008, **27**, 4475.
- 11 S. J. Kim, H. J. Reibenspies and Y. M. Darensbourg, *J. Am. Chem. Soc.*, 1996, **118**, 4115.
- 12 (a) E. Baciocchi, D. T. Giacco, O. Lanzalunga and A. Lapi, *J. Org. Chem.*, 2007, **72**, 9582; (b) C. Huang, S. Gou, H. Zhu and W. Huang, *Inorg. Chem.*, 2007, **46**, 5537; (c) K. Pramanik, U. Das, B. Adhikari, D. Chopra and H. Stoeckli-Evans, *Inorg. Chem.*, 2008, **47**, 429; (d) D. Shimizu, N. Takeda and N. Tokitoh, *Chem. Commun.*, 2006, 177.
- 13 (a) S. Pal, D. Das, C. Sinha and C. H. L. Kennard, *Inorg. Chim. Acta*, 2001, **313**, 21; (b) B. Sarkar, R. Hübner, R. Pattacini and I. Hartenbach, *Dalton Trans.*, 2009, 4653.
- 14 K. G. Rauth, S. Pal, D. Das, C. Sinha, M. Z. A. Slawin and D. J. Woollins, *Polyhedron*, 2001, **20**, 363.
- 15 R. R. Kapre, E. Bothe, T. Weyhermüller, D. S. George and K. Wieghardt, *Inorg. Chem.*, 2007, **46**, 5642.
- 16 (a) O. S. Wenger, S. García-Revilla, H. U. Güdel, H. B. Gray and R. Valiente, *Chem. Phys. Lett.*, 2004, **384**, 190; (b) M. Textor and H. R. Z. Oswald, *Z. Anorg. Allg. Chem.*, 1974, **407**, 244; (c) G. T. Morgan and F. H. Burstall, *J. Chem. Soc.*, 1934, 965.
- 17 (a) N. Hucher, B. Decroix and A. Daïch, *J. Org. Chem.*, 2001, **66**, 4695; (b) A. L. W. van Otterlo, L. G. Morgans, D. S. Khanye, A. A. B. Aderibigbe, P. J. Michael and G. D. Billing, *Tetrahedron Lett.*, 2004, **45**, 9171.
- 18 N. Campbell, W. A. Henderson and J. D. Taylor, *J. Chem. Soc.*, 1953, 1281.
- 19 S. Goswami, R. N. Mukherjee and A. Chakravarty, *Inorg. Chem.*, 1983, **22**, 2825.
- 20 C. Lee, W. Yang and R. G. Parr, *Phys. Rev. B: Condens. Matter*, 1988, **37**, 785.
- 21 (a) D. Andrae, U. Haeussermann, M. Dolg, H. Stoll and H. Preuss, *Theor. Chim. Acta*, 1990, **77**, 123; (b) P. Fuentealba, H. Preuss, H. Stoll and L. V. Szentpaly, *Chem. Phys. Lett.*, 1982, **89**, 418.
- 22 M. J. Frisch, G. W. Trucks, H. B. Schlegel, G. E. Scuseria, M. A. Robb, J. R. Cheeseman, J. A. Montgomery, Jr., T. Vreven, K. N. Kudin, J. C. Burant, J. M. Millam, S. S. Iyengar, J. Tomasi, V. Barone, B. Mennucci, M. Cossi, G. Scalmani, N. Rega, G. A. Petersson, H. Nakatsuji, M. Hada, M. Ehara, K. Toyota, R. Fukuda, J. Hasegawa, M. Ishida, T. Nakajima, Y. Honda, O. Kitao, H. Nakai, M. Klene, X. Li, J. E. Knox, H. P. Hratchian, J. B. Cross, V. Bakken, C. Adamo, J. Jaramillo, R. Gomperts, R. E. Stratmann, O. Yazyev, A. J. Austin, R. Cammi, C. Pomelli, J. Ochterski, P. Y. Ayala, K. Morokuma, G. A. Voth, P. Salvador, J. J. Dannenberg, V. G. Zakrzewski, S. Dapprich, A. D. Daniels, M. C. Strain, O. Farkas, D. K. Malick, A. D. Rabuck, K. Raghavachari, J. B. Foresman, J. V. Ortiz, Q. Cui, A. G. Baboul, S. Clifford, J. Cioslowski, B. B. Stefanov, G. Liu, A. Liashenko, P. Piskorz, I. Komaromi, R. L. Martin, D. J. Fox, T. Keith, M. A. Al-Laham, C. Y. Peng, A. Nanayakkara, M. Challacombe, P. M. W. Gill, B. G. Johnson, W. Chen, M. W. Wong, C. Gonzalez and J. A. Pople, *GAUSSIAN 03 (Revision B.01)*, Gaussian, Inc., Wallingford, CT, 2004.
- 23 *NBO Version 3.1*, E. D. Glendenning, A. E. Reed, J. E. Carpenter and F. Weinhold.
- 24 (a) R. Bauernschmitt and R. Ahlrichs, *Chem. Phys. Lett.*, 1996, **256**, 454; (b) R. E. Stratmann, G. E. Scuseria and M. J. Frisch, *J. Chem. Phys.*, 1998, **109**, 8218; (c) M. E. Casida, C. Jamorski, K. C. Casida and D. R. Salahub, *J. Chem. Phys.*, 1998, **108**, 4439.
- 25 (a) V. Barone and M. Cossi, *J. Phys. Chem. A*, 1998, **102**, 1995; (b) M. Cossi and V. Barone, *J. Chem. Phys.*, 2001, **115**, 4708; (c) M. Cossi, N. Rega, G. Scalmani and V. Barone, *J. Comput. Chem.*, 2003, **24**, 669.
- 26 N. M. O'Boyle, A. L. Tenderholt and K. M. Langner, *J. Comput. Chem.*, 2008, **29**, 839.
- 27 (a) G. M. Sheldrick, *Acta Crystallogr., Sect. A: Found. Crystallogr.*, 1990, **46**, 467; (b) G. M. Sheldrick, *SHELXL 97. Program for the refinement of crystal structures*, University of Göttingen, Göttingen, Germany, 1997.